X-RAY ABSORBER DESIGN AND CALCULATIONS FOR THE EBS STORAGE RING

F. Thomas[1], J.C. Biasci, D. Coulon, Y. Dabin, T. Ducoing, F. Ewald, E. Gagliardini, P. Marion
European Synchrotron Radiation Facility (ESRF), Grenoble, France
[1] also at Institut Laue-Langevin (ILL), Grenoble, France

Abstract

The Extremely Brilliant Source (EBS) of the ESRF will hold new type of X-Ray absorbers: a new material will be used (CuCr1Zr suggested by [1]) together with a novel design integrating:

- Conflat (CF) flange machined in the absorber body. No weld, no braze.
- Optimized toothed surface profile, reducing the induced thermal stresses.
- Fluorescence Compton and Rayleigh scattering integrated blocking shapes.
- Concentric cooling channels.

A brief overview of the new design and concepts for toothed absorbers will be given.

The presentation will then focus on thermal-mechanical absorber calculations, combining both Computational Fluid Mechanics (CFD) and Finite Elements Analysis (FEA). The calculations were made using the ANSYS packages [2, 3].

The calculations and calculation process will be discussed as well as the design criteria chosen by the team.

The CFD calculations will show that an effective heat transfer coefficient between the water and the copper part can be estimated for concentric cooling channels as well as the pressure drop through the absorber.

Finally, the stress analysis will be emphasized. The type of stresses (tensile, compressive or shear) and their nature (primary or secondary) will be linked to the choice of design criteria.

INTRODUCTION

The ESRF took the strategic decision to make most if not all the X-Ray absorbers of the new EBS storage ring in CuCr1Zr copper alloy instead of classical Cu OFE [4] or Glidcop® AL-15 [5]. In order to reduce the risk of using a new material, we designed absorbers in a way that they work always in the purely elastic regime.

The first paragraph will be a brief overview of the new design and concepts used for toothed absorbers – machined CF flange, toothed scattering blocking shape and concentric cooling channels.

In the second paragraph, we will discuss the CFD model used to determine an effective heat transfer coefficient of 15 kW/m^2/K per cooling channel for a flow rate of 4.24 l/min together with an estimated pressure drop of $\Delta p \sim$ 0.3 bar.

The third paragraph will show thermal and mechanical calculation results of one of the new absorbers: the 2 cooling channels, single jaw, ABS-CH9-1-2 horizontal absorber. The stress analysis will be detailed and linked to stress design criteria.

BRIEF OVERVIEW

In the EBS, the toothed absorbers will have to absorb normal power incident densities up to 110 W/mm^2. In order to spread out the heat load on larger surfaces, one can make triangular toothed surfaces, reducing the power density by $\sin(\beta).\tan(\alpha)$, 2β being the top angle of the triangular tooth and α the tilt angle of the teeth base relative to the beam, i.e. the grazing angle if they were no teeth – see fig. 1. In our case, optimization between large spreading surfaces, implementation in the vacuum chamber, standardization and machinability leads to a 2β angle of 45° and an α angle around 10° (absorber dependent due to geometrical constraints), reducing the power density deposited by ~ 90-95% (theoretically).

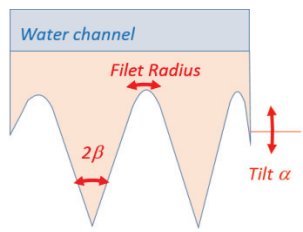

Figure 1: Relevant parameters for an absorber's jaw

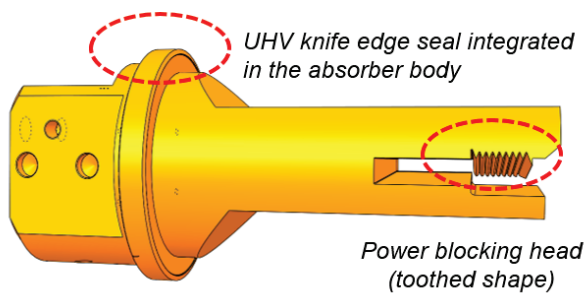

Figure 2: Toothed horizontal absorber overview

Figure 2 emphasizes the innovating design choices made for the EBS absorbers: CF knife edge machined in the absorber body, single jaw absorbers with a longer tooth at the right end of the jaw.

We made the calculations assuming that the angular misalignment was 1.5°, 0.5° from the angular divergence of the X-ray beam and keeping 1° safety margin.

ISBN 978-3-95450-188-5

A majority of the absorber's calculations were made 3 times with the beam centered on the jaw and with a beam offset by ± 2 mm in height. Shifting the beam by ± 2 mm is a second order modification compared to rotating the absorber by 1.5°.

a) Face Numbering

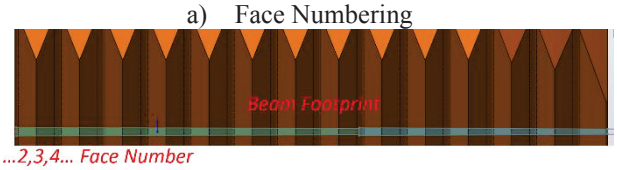

b) Heat Load

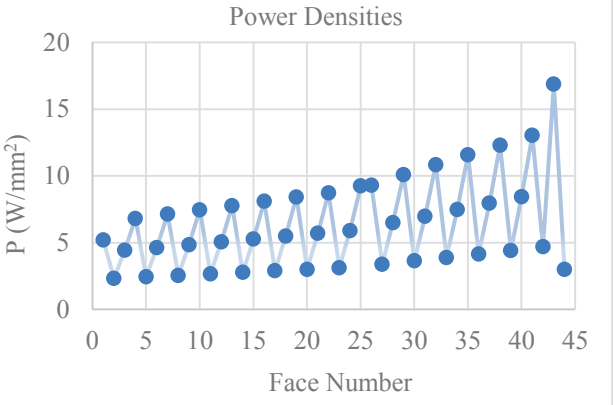

Figure 3: Heat load per face ABS-CH9-2-2

Figure 3 shows surface numbering (a) and heat load per face (b) for one of the toothed absorber: ABS-CH9-2-2, the vertical absorber of the vacuum chamber 9. Faces 1,4,7...38,41 are 0.32 mm in radius connecting filets between the teeth, the other faces being the teeth faces: 2,5,8… are the left faces viewed by the beam and 3,6,9… the right faces. The 1.5° misalignment induces large left right asymmetry (a factor of 2) in the heat load between the 2 faces of each tooth. Nevertheless, the power density is still smaller (but close) on flat faces that on connecting filets. In other words, we optimized the pair tooth angle – connecting filet radius to handle roughly the same maximum power density on both objects.

Last tooth is made longer (and named the super tooth, see fig.2). A flat face is put below the jaw. Both objects are fluorescence, Compton and Rayleigh scattering blockers and their efficiency has been estimated at ~ 90%. Even if they make the design and machining more complicated, they avoid the cooling of vacuum chambers with water.

Complementary details about the design of theCuCr1Zr EBS absorbers are given in [6]. One of the main advantages is that the material is hard enough – Brinell hardness larger than 125 HB – and isotropic enough to machine the CF flange directly on the CuCr1Zr part, making an absorber with no weld and no braze therefore no assembling problem.

CFD MODEL

Surprisingly, CFD has not been widely used in the past for absorber heat transfer calculations. Even in recent literature (see for example [1, 7, 8]), authors refer to a heat transfer film coefficient value that varies from 10 to 20 kW/m^2/K with no or little precisions concerning the cooling channel dimensions and the flow rate.

For the EBS absorbers, we decided to study a generic case of concentric cooling channels with a water flow rate (2.5 m/s ~ 4.24 l/min) that will be eventually used, in order to extract both the average heat transfer coefficient per channel and the total pressure drop.

All CFD calculations were made using the k-ε turbulence model with automatic wall functions [9]. A sensitivity study has been performed for the turbulence model.

Hydraulic Model

Each concentric cooling channel consists in a Φ6x8 mm stainless steel 316L tube inserted Φ10 mm hole in the bulk of the absorber. The channel cross section is roughly the same inside the tube than between the tube and the copper alloy hole (~ 28 mm^2). The extremity of the tube is in contact with the bottom of the hole and machined with two apertures of sections 2x14 mm^2 for the water to pass between the inside of the tube and the annular channel. The tube is centered in the hole by small spacers. The geometry was chosen for its simplicity and for its compactness.

Calculations are performed on ½ of the model, due to symmetry.

Figure 4 shows the pressure drop across two consecutive cooling channels. The water enters the model at the inner of the top left hand side stainless steel tube, going down, then the flow reverses at the bottom of the tube and goes up in the gap between the tube and the bulk of the absorber. The water flows horizontally in the green part and then flows down in the gap between the right hand side tube and the bulk. At the bottom of the hole, there is a second flow reversal and the water exits through the inner of the right hand side stainless steel tube, going up.

Gravity is oriented in the –y direction (downward).

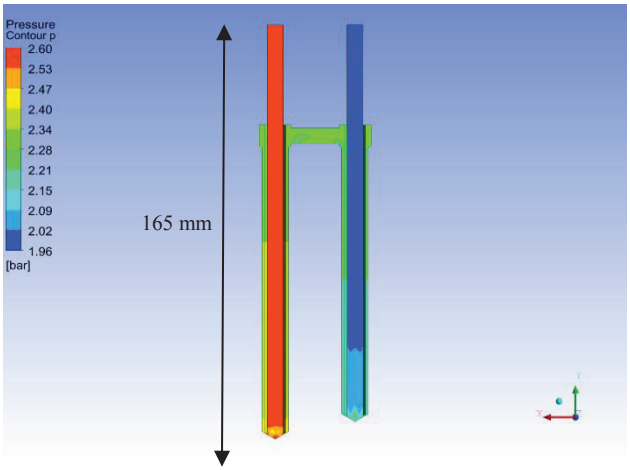

Figure 4: Pressure drop across two consecutive coaxial cooling channels.

Pressure drop is found to be $\Delta p \sim 0.6$ bar for two channels - see fig. 4. As the cross section is kept the same along all the cooling path, the specific pressure loss is due to changes on the flow direction and friction along tubes. One sees also on the contour plot that the total pressure drop is dominated by specific pressure losses. A rough estimate per channel would give:

- Frictional loss coefficient: $\xi = 0.04 \times 350/6 = 2.3$.
- Specific loss coefficient: $\xi > 5$ [10].
- Gravity: no.

The total loss coefficient is found to be $\xi_{tot} > 7.3$ with the rough estimate and $\xi_{tot} = 10$ with the CFD result.

From this study (and from other studies too) we decided to keep the $\Delta p \sim 0.3$ bar per cooling channel at 4.24 l/min ($\xi_{tot} = 10$) as the design value for all concentric cooling absorbers. Note that as the flow is turbulent, the pressure drop varies essentially with the square of the flow rate.

Thermal Hydraulic Model

The thermal-hydraulic model is a simplified absorber with a single cooling channel (see fig. 4). Calculations are performed on ¼th of the model, due to symmetries. In this model, the extremity of the tube has four apertures of sections 4x7 mm^2 to be consistent with the symmetry.

Figure 5 shows the calculated heat transfer coefficient. The coefficient varies in the range 6-46 kW/m^2/K for an average value of 18 kW/m^2/K.

In addition to the generic absorber, thermal-hydraulic calculations have been performed on two more absorbers, giving comparable results. We decided to take a conservative design value of 15 kW/m^2/K for calculations for which there was no time to make a complete fluid-structure model. The design value is conservative because:

- Its value is lower than the calculated value.
- Using an average value is conservative: the heat transfer coefficient is bigger than its average in the region where the heat flux is large, i.e. close to the region where the beam is absorbed.

In other words: the flow reversal induces a significant pressure drop, but at the same time, increases the heat transfer coefficient significantly.

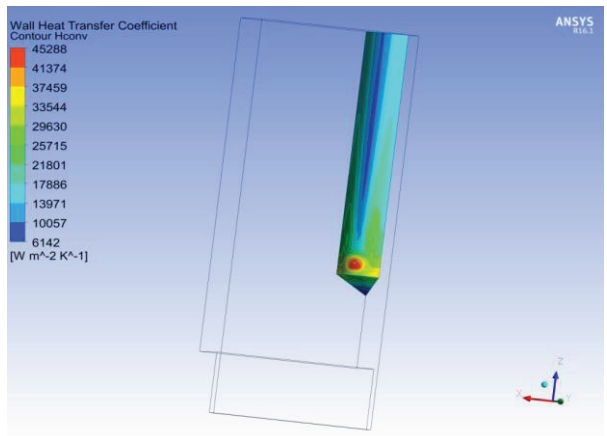

Figure 5: Heat Transfer Coefficient of a Cooling Channel.

Finally, we verified with a parametric calculation that the average heat transfer coefficient h varies linearly with flow velocity v (or flow rate), in the range 0-5 m/s. This result is not trivial: using the Dittus and Boelter correlation [11] would have led to $h \propto v^{0.8}$. But again, the space saving concentric cooling geometry is somehow exotic to address a heat transfer problem.

THERMAL-MECHANICAL MODELS

Specified Mechanical Properties

Using off-the-shelf CuCr1Zr would be risky as the thermal and mechanical properties may vary significantly from one batch to another, as well as purity, grain size, inclusions, etc... In other words, the EN standard CW106C was too permissive to guaranty the supplying of material with high enough thermal, mechanical and chemical properties.

The ESRF took the decision to write a full specification [12] to focus on material definition for the call for tender (CFT), making the CFT more challenging for suppliers. In particular, at 250°C, the material should have a yield strength value larger than 280 MPa, an elongation at break larger than 8%, a Brinell hardness larger than 125 HB and a thermal conductivity larger than 300 W/m/K.

Elastic Analysis Stress Criteria

During the past 10 years, several different criteria have been proposed for the dimensioning of X-Ray absorbers and the acceptable maximum stress for Copper and Glidcop® submitted to thermal stresses and to a large number of fatigue cycles [13-17]. Completing and updating the survey made by [13], we have built the table 1. In the table, S_y refers to the yield strength,

ISBN 978-3-95450-188-5

S_F to the fatigue strength, σ_{VM} to the Von-Mises equivalent stress, σ_1 and σ_3 to the maximum and minimum principal stress respectively and τ_{Max} to the maximum shear stress.

Table 1: Thermal and Stress Analysis Criteria

Accelerator	Maximum Temperature	Maximum Stress / Strain
ALBA	400° (Glidcop®)	0.2% strain (10^5 cycles)
ANKA, SLS	(Copper)	0.2% strain (10^4 cycles)
APS	541° (Copper) 405° (Glidcop®)	$2.S_y$, S_F (10^5 cycles) Fatigue Model
DIAMOND	(Copper)	0.5% peak strain 0.1% bulk strain
ESRF	$T_{Melt}/2$ (All Materials)	$\sigma_{VM} < S_y$
ESRF, EBS	250° (CuCr1Zr)	$\sigma_1 < S_y = 280MPa$ $\sigma_3 > -S_y$ $\tau_{Max} < S_y/2$
SOLEIL	(All Materials)	$\sigma_{VM} < 0.75.S_y$
SPRING-8	(All Materials)	Fatigue Model

Many authors propose acceptable stresses higher than the material yield strength. In comparison, the ESRF-EBS criteria look conservatives, but we had to manage the fact that:

- Around 400 absorbers will be mounted in the storage ring for 20 years.
- We should be conservative as we deal with a new material.

Toothed absorbers are often different in the nature of the stress. Due to the teeth, the maximum principal (tensile) and maximum shear stress reach high values as in flat face absorbers, the stress is dominated by the minimum principal (compressive) stress. Those tensile and shear stresses impact more the robustness – in case of cracks in the absorber for example - than a pure compressive stress.

Most if not all the stresses in absorbers are secondary stresses as they are due to shape adaptation of the part and not to an external force and/or pressure.

If one wants to use ASME like criteria for elastic analysis and secondary stresses, the criterion would be in this case $\tau_{Max} < S_y$ [18]. In other words, in the ASME frame, for secondary stresses, we have a safety factor of 2 in the elastic analysis stress criteria.

ABS-CH9-1-2 Horizontal Absorber

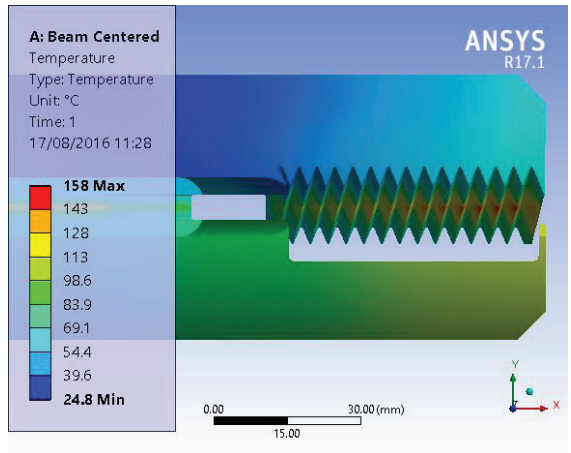

Figure 6: Temperature Plot CH9-1-2 Absorber.

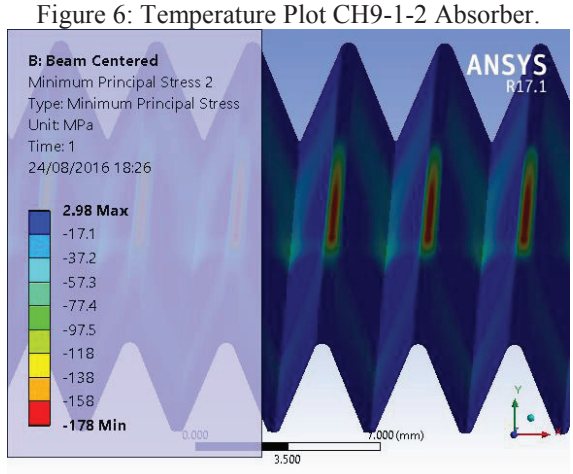

Figure 7: Minimum Principal Stress CH9-1-2 Absorber.

The ABS-CH9-1-2 is a 51 faces, 16 teeth crotch absorber with a total heat load of 3373.3 W.

The thermal load per face is similar to the one shown in figure 2. The calculations where made with a 1.5° misalignment and a heat transfer coefficient of 15 $kW/m^2/K$, those choices being explained in paragraph 1 and 2.

The maximum temperature is found to be 158° C at the tooth n°15 as shown in figure 6. According to our criteria, the dimensioning stress (together with the maximum shear stress) is the minimum principal stress shown in figure 7. Its minimum value is -178 MPa in the filet connecting tooth n°8 and tooth n°9. We found a maximum principal stress peak value of 116 MPa and a maximum shear stress peak value of 89 MPa.

This example shows what we observed on roughly every absorber: the connecting filet cannot be optimized independently from the teeth:

- Using a smaller filet radius would increase the tensile and shear stresses on adjacent teeth; the teeth needs loose connections one to each other in order to expand with no stress when warming.

- Using a larger filet radius would increase furthermore the compressive stress in the filet as the "average" grazing angle in the filet would increase.

Again, we decided to have all the EBS storage ring toothed absorbers with 45° tooth angle and 0.32 mm connecting filet radius.

Finally, this example points out a very fundamental difference between frontal and toothed absorbers:

- Frontal absorbers are large bulky parts with very localized heat loads, their thermal-mechanical behavior is plane ***strain*** driven.
- At the other end of the spectrum, focusing lenses, for example, are light thin parts, their thermal-mechanical behavior is plane ***stress*** driven.

Toothed absorbers with small teeth and loosed teeth connections are transition objects in between, plane strain dominated close to the beam and plain strain dominated in the rest of the jaw. Depending on the design, the plain stress or the plain stress may be the dimensioning factor, or, as in ABS-CH9-1-2, both play a role.

CONCLUSION

The ESRF decided to use a new material (CuCr1Zr) for most of its EBS storage ring absorbers. To turn this decision into a success, we decided to be conservative in term of design and calculation criteria:

- The position and angle tolerances are loose: ± 2 mm in height and ± 1° in angle.
- The maximum temperature for the absorber should be less than 250°C.
- The maximum principal stress peak value should be less than 280 MPa, and the maximum shear stress peak value less than 140 MPa.
- The minimum principal stress peak value should be more than -280 MPa.

All CuCr1Zr storage ring absorbers have been calculated so far and they all comply to the design and calculation criteria.

In addition to that, we studied extensively the efficiency of a new type of cooling channel, with a concentric design. We found that the effective heat transfer coefficient for such a channel is larger than 15 $kW/m^2/K$ for a water velocity of 2.5 m/s and varies linearly with the water velocity. The cooling channel geometry leads to a specific pressure loss coefficient of 10.

Finally, the hardness of the material and prototypes of CF flanges in CuCr1Zr [6] validate the fact that one can design a storage ring absorber as a single mechanical part with no braze and no weld, thus reducing the risk of failure/leaks and the complexity of manufacturing them.

REFERENCES

[1] S. Sharma, "A Novel Design of High Power Masks and Slits", Proc. of MEDSI2014, Australia (2014).

[2] ANSYS CFX, http://www.ansys.com/Products/Fluids/ANSYS-CFX

[3] ANSYS Mechanical Enterprise, http://www.ansys.com/Products/Structures/ANSYS-Mechanical-Enterprise

[4] Oxygen-free copper Wikipedia, https://en.wikipedia.org/wiki/Oxygen-free_copper

[5] Wikipedia Glidcop, https://en.wikipedia.org/wiki/Glidcop

[6] E. Gagliardini *et al.*, "A new generation of X-ray absorbers for the EBS storage ring", poster session, MEDSI2016, Barcelona, Spain, this conference.

[7] L. Zhang, J.C. Biasci and B. Plan, "ESRF Thermal Absorbers: Temperature, Stress and Material Criteria", Proc. of MEDSI2002, U.S.A. (2002).

[8] C.K. Kuan *et al.*, "Thermal Analysis of Absorbers for the 3 GeV TPS", Proc. of MEDSI2006, Japan (2006).

[9] CFD Online, http://www.cfd-online.com/Wiki/Two_equation_turbulence_models

[10] I.E. Idelchick, "Handbook of Hydraulic Resistance", 4th Revised and Augmented Edition, Ed. Begell House, Inc., 2007, p 469, ISBN: 978-1-56700-251-5.

[11] R.H.S. Winterton, "Where did the Dittus and Boelter equation come from?", Int. J. Heat Mass Transfer, Vol. 41, Nos 4-5, pp.809-810, 1998.

[12] ESRF / ENG / 15-09

[13] M. Quispe *et al.*, "Development of the Crotch Absorber for ALBA storage ring", Proc. of MEDSI2008, Canada (2008).

[14] S. Takahashi *et al.*, "Prediction of fatigue life of high-heat load components made of oxygen-free copper comparing with Glidcop", J. Synchrotron Radiat., 20 (Pt 1), pp.67-73, Jan. 2013.

[15] S. Takahashi *et al.*, "Reconsideration of Design Criteria for High-Heat-load Components at Spring-8 Front Ends", Proc. of MEDSI2006, Japan (2006).

[16] J. Colins *et al.*, "Results from Studies of Thermomechanically- Induced Fatigue in Glidcop®", Proc. of MEDSI2014, Australia (2014).

[17] L. Zhang, "Absorber Conceptual design and optimisation", ESRF Technical Report (2014).

[18] M.H. Jawad and J.R. Farr, "Structural Analysis and Design of Process Equipment", Ed. John Wiler & Sons, 1984, p 20 and p 32, ISBN: 0-471-09207-X.

ISBN 978-3-95450-188-5